Shape-Only Granulometries and Gray-Scale Shape Filters

Urbach, E.R.; Wilkinson, M.H.F.

Published in:
EPRINTS-BOOK-TITLE

Publication date:
2002

SHAPE-ONLY GRANULOMETRIES AND GRAY-SCALE SHAPE FILTERS

E. R. Urbach, M. H. F. Wilkinson
Institute for Mathematics and Computing Science,
University of Groningen, P.O. Box 800, 9700 AV, Groningen,
The Netherlands

Abstract Multiscale methods which provide a decomposition of an image based on scale have many uses in image analysis. One class of such methods from mathematical morphology is based on *size distributions* or *granulometries*. In this paper a different type of image decomposition based on *shape* but not scale is proposed. Called a *shape granulometry* or *shape distribution*, it is built from a family of morphological thinnings, rather than openings as in the case of size distributions. An implementation based on scale invariant attribute thinnings is presented, and an example of an application is shown.

Keywords: Multi-scale analysis, connected filters, granulometries, attribute thinnings.

1. Introduction

Size distributions or granulometries form an important class of multi-scale tools in mathematical morphology. They were initially introduced by Matheron [5], and have found many applications (for a recent review of granulometries see [10]). Intuitively, a size distribution can be considered as a set of sieves of different grades, each allowing details of certain size classes to pass. They can be used to classify or extract image details of different size classes (scales). Usually, the width of each detail is the relevant size criterion. Apart from their use in image filtering, size distributions can be used to generate morphological pattern spectra, which summarize the action of a size distribution on a particular image in a single, 1-D array [6, 7].

More formally, a size distribution consists of an ordered set of operators each of which convert an image to a new image in which features smaller than a particular size are absent. These filters must be idempotent, anti-extensive, and increasing, which means they must be *openings*. Many, though not all [6, 7], types of opening can be used as granulometries.

 ISBN 0 643 06804 X

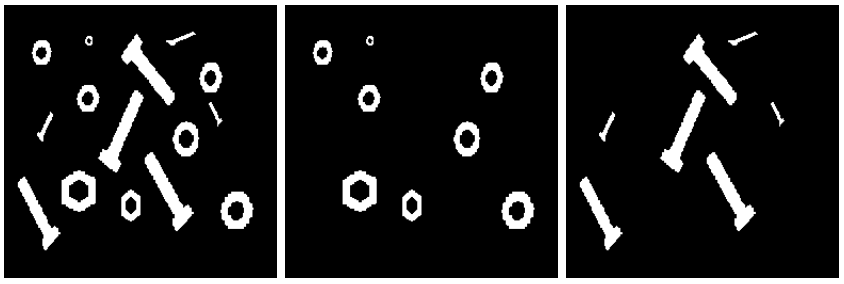

Figure 1. Decomposition of binary image of nuts and bolts of different sizes into different shape classes: (left) original image; (middle) attribute thinning with criterion: number of holes > 0; (right) difference between (left) and (middle).

Fairly recently Breen and Jones [3] proposed a new type of size distribution based on attribute openings, which belong to the class of connected filters. These allow the use of many size criteria other than width, such as area, length of the diagonal of the minimum enclosing rectangle, moment of inertia, etc., to define the "grades" of the morphological sieves. They also put forward the idea of attribute thinnings, which allow image filtering based on shape, rather than size criteria. Fig. 1 shows an example. Their work is related to that of Bangham et al. [1, 2], who also proposed the use of connected set openings and closings for image decompositions.

In this paper we extend these ideas to *shape granulometries* or *shape distributions*, which are ordered sets of *shape filters*. We introduce the latter as scale invariant thinnings, which are idempotent, anti-extensive, but not increasing. They allow extraction of pattern spectra based on shapes, rather than sizes of details, which could be useful if the type of details searched for are characterized by shape rather than size. This might be the case when trying to find e.g. human faces in natural images. Because the distance to the camera may vary, scale may carry less information about the presence of certain objects than shape. An example of a decomposition of a binary image based on shape rather than size is shown in Fig. 1, where the nuts are separated from the bolts based on the number of holes.

In this paper a theory of shape distributions is proposed, and the case of attribute shape distributions is dealt with in detail. Furthermore, a criterion for decomposition of grey-scale images in terms of shape is proposed. It is shown that a new type of grey-scale attribute thinning, called a *subtractive rule* attribute thinning is needed to provide an image decomposition which meets this criterion. Finally, we briefly show some results of an application of shape filters to the problem of blood vessel enhancement in 3D angiograms, which have recently been published [11].

2. Theory

The theory of size distributions and attribute filters is presented only very briefly here. For more detail the reader is referred to [3, 4, 5, 8, 10]. In the

following discussion binary images X and Y are defined as subsets of the image domain $\mathbf{M} \subset \mathbf{R}^n$ (usually $n = 2$), and grey-scale images are mappings from $\mathbf{M}$ to $\mathbf{R}$.

2.1 Binary size and shape distributions

Definition 1 *A binary size distribution or granulometry is a set of operators* $\{\alpha_r\}$ *with* r *from some totally ordered set* Λ *(usually* $\Lambda \subset \mathbf{R}$ *or* $\mathbf{Z}$*), with the following three properties*

$$\begin{aligned} \alpha_r(X) &\subset X && (1)\\ X \subset Y &\Rightarrow \alpha_r(X) \subset \alpha_r(Y) && (2)\\ \alpha_r(\alpha_s(X)) &= \alpha_{\max(r,s)}(X), && (3) \end{aligned}$$

for all $r, s \in \Lambda$.

Since (1) and (2) define α_r as anti-extensive and increasing, respectively, and (3) implies idempotence, it can be seen that size distributions are openings. Let us define a scaling X_λ of set X by a scalar factor $\lambda \in \mathbf{R}$ as

$$X_\lambda = \{x \in \mathbf{R}^n | \lambda^{-1} x \in X\}, \tag{4}$$

and likewise, a scaling f_λ of a grey-scale image f is defined as

$$f_\lambda(x) = f(\lambda^{-1}x) \quad \forall \lambda^{-1}x \in \mathbf{M}. \tag{5}$$

An operator ϕ is said to be *scale invariant* if

$$\phi(X_\lambda) = (\phi(X))_\lambda \quad \text{or} \quad \phi(f_\lambda) = (\phi(f))_\lambda \tag{6}$$

for all $\lambda > 0$. A scale invariant operator is therefore sensitive to shape rather than to size. Using these notions we define shape operators and shape filters.

Definition 2 *A shape operator is an image operator which is scale, rotation and translation invariant. A shape operator which is idempotent is a shape filter.*

In the digital case, pure scale invariance will be harder to achieve due to discretization artefacts, but a good approximation may be achieved.

Definition 3 *A binary shape distribution is a set of operators* $\{\beta_r\}$ *with* r *from some totally ordered set* Λ*, with the following three properties*

$$\begin{aligned} \beta_r(X) &\subset X && (7)\\ \beta_r(X_\lambda) &= (\beta_r(X))_\lambda && (8)\\ \beta_r(\beta_s(X)) &= \beta_{\max(r,s)}(X), && (9) \end{aligned}$$

for all $r, s \in \Lambda$ *and* $\lambda > 0$.

Thus, a shape distribution consists of operators which are anti-extensive, and idempotent, but not necessarily increasing. Therefore, these operators are not

openings, but have the same properties as the attribute thinnings defined by Breen and Jones [3] (these are discussed in section 2.2). To exclude any sensitivity to size, we add property (8), which is just scale invariance for all β_r. Extension to grey level is straightforward.

Definition 4 *A grey-scale shape distribution is a set of operators* $\{\beta_r\}$ *with* r *from some totally ordered set* Λ*, with the following three properties*

$$\begin{aligned} (\beta_r(f))(x) &\leq f(x) && (10)\\ \beta_r(f_\lambda) &= (\beta_r(f))_\lambda && (11)\\ \beta_r(\beta_s(f)) &= \beta_{\max(r,s)}(f), && (12) \end{aligned}$$

for all $r, s \in \Lambda$ *and* $\lambda > 0$.

2.2 Attribute thinnings

As stated above, shape distributions are ordered sets of scale invariant thinnings. We will now show that attribute thinnings as defined by Breen and Jones [3] can provide such sets of operators. Binary attribute thinnings are based on binary connected openings. The binary connected opening $\Gamma_x(X)$ of X at point $x \in \mathbf{M}$ yields the connected component of X containing x if $x \in X$, and $\emptyset$ otherwise. Thus Γ_x extracts the connected component to which x belongs, discarding all others. Breen and Jones then use the concept of trivial thinnings Φ_T, which use a non-increasing criterion T to accept or reject connected sets. A criterion T is increasing if the fact that C satisfies T implies that D satisfies T for all $D \supset C$. The trivial thinning Φ_T of a connected set C with criterion T is just the set C *if* C satisfies T, and is empty otherwise. Furthermore, $\Phi_T(\emptyset) = \emptyset$. The binary attribute thinning is defined as:

Definition 5 *The binary attribute thinning* Φ^T *of set* X *with criterion* T *is given by*

$$\Phi^T(X) = \bigcup_{x \in X} \Phi_T(\Gamma_x(X)) \tag{13}$$

It can be shown that this is a thinning because it is idempotent and anti-extensive [3]. The attribute thinning is equivalent to performing a trivial thinning on all connected components in the image, i.e., removing all connected components which do not meet the criterion. It is trivial to show that if the criterion T is scale invariant:

$$T(C) = T(C_\lambda) \quad \forall \lambda > 0 \wedge C \subseteq \mathbf{M}, \tag{14}$$

so are Φ_T and Φ^T. Assume $T(C)$ can be written as $\tau(C) \geq r$, $r \in \Lambda$, with τ some scale invariant attribute of the connected set C. Let the attribute thinnings formed by these T be denoted as Φ^τ_r. It can readily be shown that

$$\Phi^\tau_r(\Phi^\tau_s(X)) = \Phi^\tau_{\max(r,s)}(X). \tag{15}$$

Therefore, $\{\Phi^\tau_r\}$ is a shape distribution, since attribute thinnings are anti-extensive, and scale invariance is provided by the scale invariance of $\tau(C)$. An example can be seen in Fig. 1.

Various grey-scale generalizations of these filters have been proposed and are compared in [8]. An efficient algorithm for computing these filters based on a tree of flat zones in the image was also put forward in the same paper. Filtering is reduced to different methods of modifying this tree structure. In section 3 this algorithm and various thinnings based on different modification strategies are discussed. First we will discuss the desirable properties of these filters if they are to be used for shape decomposition of an image.

2.3 Shape decomposition

If we wish to decompose an image into its constituent components based on shape rather than size, we would intuitively require that after filtering with grey-scale attribute thinning ϕ_r^T derived from binary attribute thinning Φ_r^T, no structures which do not meet the criterion T are present in the resulting image. Moreover, the difference image $f - \phi_r^T(f)$ should only contain structures which do not meet T. Let *peak component* P_h^k at grey level h be the kth connected component of the threshold set $X_h(f)$ of image f which is defined as

$$X_h(f) = \{x \in \mathbf{M} | f(x) \geq h\}. \tag{16}$$

The intuitive requirements now mean that all peak components of $\phi_r^T(f)$ meet T, and all peak components of $f - \phi_r^T(f)$ do not. More formally

$$\Phi_r^T(X_h(\phi_r^T(f))) = X_h(\phi_r^T(f)) \tag{17}$$

and

$$\Phi_r^T(X_h(f - \phi_r^T(f))) = \emptyset \tag{18}$$

for all h.

In the next section we will show that a new extension for grey-scale attribute thinnings is needed to meet these criteria. However, it is not trivial to characterize all filters that share these properties, other than that they must be shape filters which form a shape-distribution.

3. The Max-Tree

The *Max-Tree* representation was introduced by Salembier et al [8] as a more versatile structure to separate the filtering process in three steps: construction, filtering and restitution. Jones [4] proposed a similar structure called a component tree, intended for non-flat attribute filtering and segmentation. A Max-tree is a tree where the nodes represent sets of flat zones. The Max-Tree node C_h^k consists of the subset of P_h^k with grey level h. The root node represents the set of pixels belonging to the background, that is the set of pixels with the lowest intensity in the image. The Max-Tree is a rooted tree: each node has a pointer to its parent, i.e. the nodes corresponding to the components with the highest intensity are the leaves (see Fig. 2). Hence the name Max-Tree: the leaves correspond to the regional maxima. This means that the Max-Tree can be used for attribute openings or thinnings. Conversely, a tree in which the leaves correspond to the minima is called a Min-Tree and can be used for

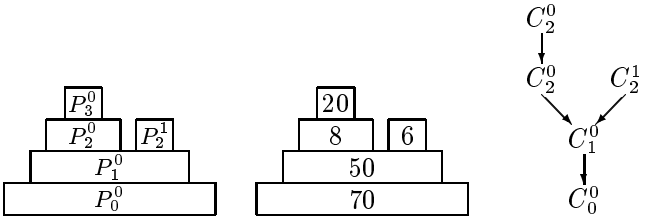

Figure 2. The peak components of a grey-scale image X (left), the corresponding attributes (middle) and the Max-Tree (right)

attribute closings or thickenings. During the construction phase, the Max-Tree is built from the flat zones of the image.

After this, the tree is processed during the filtering phase. Based on the criterion value $T(P_h^k)$ of a node C_h^k, the algorithm takes a decision on whether to preserve or to remove it. Two classes of strategies exist: (i) pruning strategies, which remove all descendants of C_h^k, if C_h^k is removed, and (ii) non-pruning strategies in which the parent pointers of children of C_h^k are updated to point at the oldest "surviving" ancestor of C_h^k. If T is non-increasing, such as perimeter or I/A^2, where I/A^2 denotes the moment of inertia divided by the square of the area, pruning strategies must either remove nodes which meet T, or leave nodes which do not. It is trivial to see that no pruning strategy can meet both decomposition properties of (17) and (18). Salembier describes four different rules for the algorithm to filter the tree: the *Min*, the *Max* the *Viterbi* and the *Direct*, decision. The first three are pruning strategies. In addition to these we introduce a new, non-pruning strategy: the *Subtractive* decision.

The decisions of these rules are as follows:

Min A node C_h^k is removed if $T(P_h^k) < r$ or if one of its ancestors is removed.

Max A node C_h^k is removed if $T(P_h^k) < r$ and all of its descendant nodes are removed as well.

Viterbi The removal and preservation of nodes is considered as an optimization problem. For each leaf node the path with the lowest cost to the root node is taken, where a cost is assigned to each transition. For details see [8].

Direct A node C_h^k is removed if $T(P_h^k) < r$; its pixels are lowered in grey level to the highest ancestor which meets T, its descendants are unaffected.

Subtractive As above, but the descendants are lowered by the same amount as C_h^k itself.

Fig. 2 shows the peak components of a 1-D grey-scale image, their attribute values, and the corresponding Max-Tree. The results of applying the Min, Max, Direct and Subtractive methods on this image with $r = 10$ are shown in Fig. 3. Which of these rules is the most appropriate depends mainly on the application, e.g. image filtering or decomposition. It can be shown that

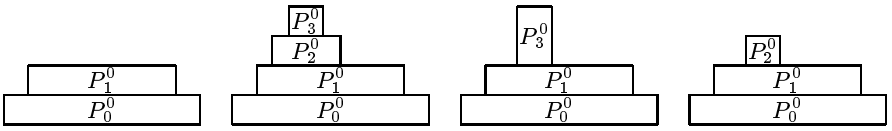

Figure 3. Result after filtering the image in Fig. 2 with (from left to right) Min, Max, Direct and Subtractive decision, with $r = 10$.

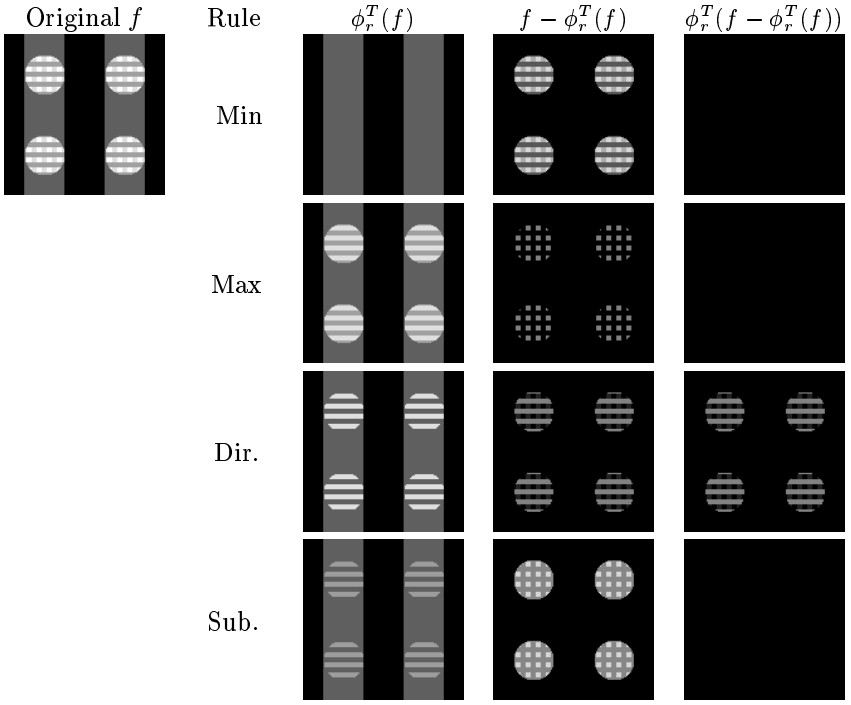

Figure 4. Grey-scale decomposition of image f using $I/A^2 > r$ thinning with $r = 1.1$ using two pruning (max and min) and two non-pruning filtering strategies. Left: original image; filtered image $\phi_r^T(f)$, difference image $f - \phi_r^T(f)$ and filtered difference image $\phi_r^T(f - \phi_r^T(f))$ are shown for all four methods (the two rightmost columns have been contrast enhanced for clarity). The min filter removes the small bars within the larger circles from the image, whereas the max pruning strategy leaves the large circles in the filtered image. Of the non-pruning rules, the direct method has the problem that the difference image contains non-compact details, as can be seen by re-filtering with ϕ_r^T (rightmost row)

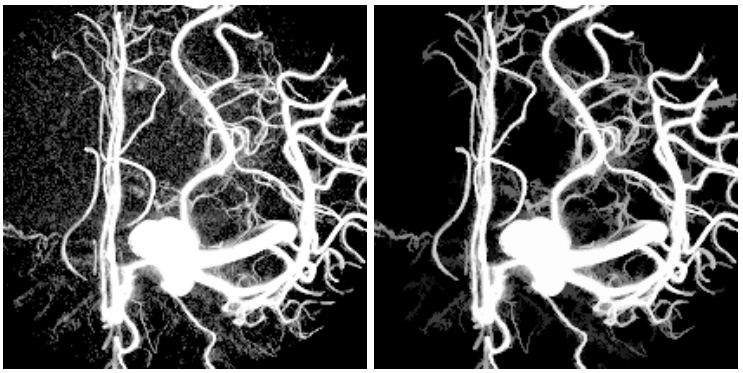

Figure 5. An application of connected set filters (grey-scale attribute thinning) to filament extraction: (left) maximum intensity projection of magnetic resonance angiogram 256^3 volume data set; (right) result using an attribute thinning as shape filter. The attribute used was $I/V^{5/3}$, with I the moment of inertia, and V the volume of a peak component; the attribute threshold was 2.0.

the subtractive rule alone satisfies both (17) and (18). Consider an image with just three nested peak components $P_3^1 \subset P_2^1 \subset P_1^1$ at grey levels 3, 2, and 1, respectively. Furthermore let $\tau(P_3^1) \geq r$, $\tau(P_2^1) < r$, and $\tau(P_1^1) \geq r$. No pruning strategy can simultaneously retain P_3^1 and P_1^1, while removing P_2^1. This means that they cannot satisfy both (17) and (18). Using the direct rule, the difference $f - \phi_r^T(f)$ will consist of a zero background with one or more connected regions at grey level 1, consisting of those pixels of P_2^1 which have grey level 2, i.e. the members of C_2^1 (which need not be connected). In general a peak component of this image may satisfy T. In the case that C_2^1 is a single connected region, this means that $\tau(C_2^1) \geq r$. In the subtractive case, the difference image consists of only those peak components which do not satisfy T. An example of these properties is shown in Fig. 4: in the case of the subtractive rule, the filtered image $\phi_r^T(f)$ contains only elongated structures, and $f - \phi_r^T(f)$ contains only compact structures.

4. Discussion

It has been shown that image decomposition using shape rather than scale is feasible through the concept of shape distributions. Furthermore, binary or grey-scale attribute thinnings constitute such shape distributions if appropriate scale invariant attributes τ are used, and the criteria have the form $\tau(C) \geq r$. In the grey-scale case, the two properties desirable for image decomposition have been formulated, and it has been shown that a new form of grey-scale attribute filtering using the subtractive rule has these properties, unlike those proposed previously.

An interesting property of shape filters is that a single shape filter is a multi-scale operator, and can be used to replace multi-scale operators in certain applications. Because multi-scale operators are typically implemented by

combining the outputs of several filters (at least one at each scale), replacing them by a single shape filter can yield considerable speed gains. These applications can be found in any area where details with given shape properties may be present at different scales. One such application concerns enhancement of blood vessels in angiograms [11]. An example is shown in Figure 5. Filamentous details of all scales were detected with a single subtractive attribute filter, in which $\tau = I/V^{5/3}$, and $r = 2$ with I the moment of inertia and V the volume. Previously, multi-scale methods using banks of oriented filters at different scales were used, requiring 10 minutes on an 8 CPU Ultrasparc-based machine for a $256 \times 256 \times 103$ volume [9]. By contrast, The 256^3 volume in Figure 5 was filtered in 42 s on a 400 MHz Pentium II [11], with the added advantage that all scales were considered, not just three as in [9].

In future work we will investigate the properties and uses of pattern spectra based on shape distributions, and on fast algorithms for their computation. Furthermore, more work is needed to see whether other shape filters besides the ones discussed exist. For example, the non-flat filters proposed by Jones [4] may provide extensions to the formalism proposed here.

References

[1] J. A. Bangham, R. Harvey, P. D. Ling, and R. V. Aldridge. Morphological scale-space preserving transforms in many dimensions. *Journal of Electronic Imaging*, 5:283–299, 1996.

[2] J. A. Bangham, R. Harvey, P. D. Ling, and R. V. Aldridge. Nonlinear scale-space from n-dimensional sieves. In *Proceedings IEEE ECCV'96*, volume 1064 of *Lecture Notes in Computer Science*, pages 189–198, 1996.

[3] E. J. Breen and R. Jones. Attribute openings, thinnings and granulometries. *Computer Vision and Image Understanding*, 64(3):377–389, 1996.

[4] R. Jones. Connected filtering and segmentation using component trees. *Computer Vision and Image Understanding*, 75:215–228, 1999.

[5] G. Matheron. *Random Sets and Integral Geometry*. John Wiley, 1975.

[6] P. F. M. Nacken. Chamfer metrics in mathematical morphology. *Journal Mathematical Imaging and Vision*, 4:233–253, 1994.

[7] P. F. M. Nacken. Chamfer metrics, the medial axis and mathematical morphology. *Journal Mathematical Imaging and Vision*, 6:235–248, 1996.

[8] P. Salembier, A. Oliveras, and L. Garrido. Anti-extensive connected operators for image and sequence processing. *IEEE Transactions on Image Processing*, 7:555–570, 1998.

[9] Y. Sato, S. Nakajima, N. Shiraga, H. Atsumi, S. Yoshida, T. Koller, G. Gerig, and R. Kinikis. 3D multi-scale line filter for segmentation and visualization of curvilinear structures in medical images. *Medical Image Analysis*, 2:143–168, 1998.

[10] L. Vincent. Granulometries and opening trees. *Fundamenta Informaticae*, 41:57–90, 2000.

[11] M. H. F. Wilkinson and M. A. Westenberg. Shape preserving filament enhancement filtering. In W. J. Niessen and M. A. Viergever, editors, *Medical Image*

Computing and Computer-Assisted Intervention, volume 2208 of *Lecture Notes in Computer Science*, pages 770–777, 2001.